



## Suppressing the rhamnogalacturonan lyase gene *FaRGLyase1* preserves RGI pectin degradation and enhances strawberry fruit firmness

Pablo Ric-Varas<sup>a</sup>, Candelas Paniagua<sup>a</sup>, Gloria López-Casado<sup>a</sup>, Francisco J. Molina-Hidalgo<sup>b</sup>, Julia Schückel<sup>c</sup>, J. Paul Knox<sup>d</sup>, Rosario Blanco-Portales<sup>b</sup>, Enriqueta Moyano<sup>b</sup>, Juan Muñoz-Blanco<sup>b</sup>, Sara Posé<sup>a</sup>, Antonio J. Matas<sup>a</sup>, José A. Mercado<sup>a,\*</sup>

<sup>a</sup> Instituto de Hortofruticultura Subtropical y Mediterránea 'La Mayora' (IHSM-UMA-CSIC), Departamento de Botánica y Fisiología Vegetal, Universidad de Málaga, 29071, Málaga, Spain

<sup>b</sup> Departamento de Bioquímica y Biología Molecular, Universidad de Córdoba, 14071, Córdoba, Spain

<sup>c</sup> Department of Plant and Environmental Sciences, University of Copenhagen, Copenhagen, Denmark

<sup>d</sup> Centre for Plant Sciences, Faculty of Biological Sciences, University of Leeds, Leeds, LS2 9JT, UK

### ARTICLE INFO

#### Keywords:

Cell wall

*Fragaria*

Fruit ripening

Fruit softening

Rhamnogalacturonan I

### ABSTRACT

Plant rhamnogalacturonan lyases (RGLyases) cleave the backbone of rhamnogalacturonan I (RGI), the “hairy” pectin and polymer of the disaccharide rhamnose (Rha)-galacturonic acid (GalA) with arabinan, galactan or arabinogalactan side chains. It has been suggested that RGLyases could participate in remodeling cell walls during fruit softening, but clear evidence has not been reported. To investigate the role of RGLyases in strawberry softening, a genome-wide analysis of RGLyase genes in the genus *Fragaria* was performed. Seventeen genes encoding RGLyases with functional domains were identified in *Fragaria* × *ananassa*. *FaRGLyase1* was the most expressed in the ripe receptacle of cv. Chandler. Transgenic strawberry plants expressing an RNAi sequence of *FaRGLyase1* were obtained. Three transgenic lines yielded ripe fruits firmer than controls without other fruit quality parameters being significantly affected. The highest increase in firmness achieved was close to 32%. Cell walls were isolated from ripe fruits of two selected lines. The amount of water-soluble and chelated pectins was higher in transgenic lines than in the control. A carbohydrate microarray study showed a higher abundance of RGI epitopes in pectin fractions and in the cellulose-enriched fraction obtained from transgenic lines. Sixty-seven genes were differentially expressed in transgenic ripe fruits when compared with controls. These genes were involved in various physiological processes, including cell wall remodeling, ion homeostasis, lipid metabolism, protein degradation, stress response, and defense. The transcriptomic changes observed in *FaRGLyase1* plants suggest that senescence was delayed in transgenic fruits.

### 1. Introduction

Fruit ripening is a complex developmental process that involves many genetic and biochemical modifications, such as the accumulation of pigments and soluble sugars, the production of aromatic compounds, or flesh softening. These changes, originally evolved to make fruits more attractive to animals for seed dispersal, and converted the fruit into an edible commodity adequate for human consumption. The rate of fruit softening is an economically important trait since this determines the length of time from harvest to retail and the shelf life at consumers' homes (Brummell et al., 2022). Strawberry (*Fragaria* × *ananassa* Duch.) belongs to the group of soft fruits characterized for their fast softening,

acquiring a melting texture in a few days after full ripeness.

The disassembly of the primary cell walls, the dissolution of the middle lamella, and the reduction in cell turgor have been identified as the main factors triggering fruit softening (Brummell, 2006; Wang et al., 2018; Posé et al., 2019). At the cell wall level, the most pronounced ripening-associated changes occur in the pectin fraction, involving the depolymerization and solubilization of homogalacturonan (HG), the demethylation of HG and the loss of arabinan and galactan side chains from rhamnogalacturonan I (RGI) (Brummell et al., 2022). It is assumed that pectin remodeling reduces wall strength and cell adhesion, promoting textural changes. The critical role of pectins in fruit softening has been assessed by functional analysis of genes encoding pectinase

\* Corresponding author.

E-mail address: [mercado@uma.es](mailto:mercado@uma.es) (J.A. Mercado).

<https://doi.org/10.1016/j.plaphy.2023.108294>

Received 27 October 2023; Received in revised form 1 December 2023; Accepted 18 December 2023

Available online 23 December 2023

0981-9428/© 2023 The Authors.

Published by Elsevier Masson SAS. This is an open access article under the CC BY-NC-ND license (<http://creativecommons.org/licenses/by-nc-nd/4.0/>).

enzymes. Thus, transgenic down-regulation of genes encoding pectate lyase or polygalacturonase, both enzymes depolymerizing the HG backbone, or  $\beta$ -galactosidase, an enzyme that releases galactose from RGI side chains, decreased softening and extended shelf life in fruits with contrasting textural properties, including a soft fruit as strawberry (Jiménez-Bermúdez et al., 2002; Atkinson et al., 2012; Uluşik et al., 2016; Paniagua et al., 2020; López-Casado et al., 2023).

Rhamnogalacturonan I (RGI) polymers are highly ramified pectins composed of a backbone of the disaccharide rhamnose (Rha)-galacturonic acid (GalA), partially substituted at O-4 or O-3 positions of Rha residues by arabinan, galactan or arabinogalactan side chains (Yapo, 2011). This pectin domain, also known as hairy pectin, accounts for 5–45% of cell wall pectins, depending on the source and extraction method (Yapo, 2011). How the different pectin domains are interconnected *in muro* is unknown. The most accepted model suggests that pectins are constituted by a linear HG backbone interspersed with Rha residues and alternated at regular intervals with RGI, xylogalacturonan, and rhamnogalacturonan II domains (De Vries et al., 1982). Alternative models attribute greater importance to the RGI and postulate that this pectin domain functions as a scaffold to which other pectins are covalently linked as side chains (Vincken et al., 2003; Yapo, 2011). As previously commented, RGI remodeling during fruit ripening involves the loss of galactan and arabinan side chains, and this process has been associated with fruit softening. However, the role of enzymes degrading the RGI backbone has received little attention. Rhamnogalacturonan hydrolases (EC 3.2.1.171–3.2.1.174) and lyases (EC 4.2.2.; RGLs) can potentially degrade the backbone of RGI. In plants, only RGL genes have been described. These enzymes are found in four polysaccharide lyase (PL) families (CAZy database, [www.cazy.org](http://www.cazy.org)): PL11 and PL9, containing RG endo-lyases of fungal and bacterial origin; PL26, bacterial and fungal exo-lyases; and PL4, comprising most eukaryotic endo-lyases of fungal and plant origin. RGLs from the PL4 family contain three domains tightly packed (McDonough et al., 2004). The N-terminal domain (PF06045) is the largest and contains the catalytic site. The central domain (PF14686), a fibronectin type III-like domain, and the C-terminal domain (PF14683), a carbohydrate-binding module, are probably involved in binding to the carbohydrate substrate (McDonough et al., 2004).

Several experimental pieces of evidence support the role of RGLs in cell wall remodeling during fruit softening. Thirteen genes encoding RGLs have been described in tomato (Berumen Varela et al., 2017). Expression of one of them, *Solyc11g011300*, under the control of the constitutive promoter CaMV35S resulted in higher transgene expression level during tomato fruit growth but lower mRNA level and protein activity at ripening stages, supposedly due to a co-suppression effect (Ochoa-Jiménez et al., 2018). Transgenic tomato fruits were firmer and displayed a longer shelf life than control (Ochoa-Jiménez et al., 2018). In strawberry, Molina-Hidalgo et al. (2013) identified an RGL gene, *FaRGLyase1*, whose expression increased as the fruit ripened. Transient silencing by agroinfiltration into fruit receptacles reduced the degradation of the middle lamella, suggesting a role of this gene in strawberry softening. In *F. chiloensis*, one of the progenitors of the cultivated strawberry, the expression pattern of *FchRGL1* has also been related with fruit softening (Méndez-Yañez et al., 2020). To gain insight into the role of RGLs in the cell wall remodeling process associated with fruit softening, a genome-wide analysis of RGLyase genes in *Fragaria* has been performed in this research. Additionally, transgenic strawberry plants with *FaRGLyase1* down-regulated by RNAi were generated, and their fruits were characterized at the cell wall composition and transcriptomic levels. The results indicate that the *FaRGLyase1* gene participates actively in the degradation of RGI and strawberry fruit softening.

## 2. Materials and methods

### 2.1. Plant material

Strawberry plants (*Fragaria* × *ananassa* Duch.) cv. ‘Chandler’

obtained by runner propagation were used. Plants were grown in 22 cm pots containing peat moss, sand, and perlite (6:3:1) and cultured in a confined greenhouse with a cooling system to maintain the maximum temperature below 30 °C. ‘Chandler’ plants micropropagated in a medium containing N30K mineral formulation, MS microelements and vitamins, and 2.21  $\mu$ M kinetin (Barceló et al., 1998) were used for genetic transformation.

### 2.2. Identification of RGL genes in *fragaria*

The seed sequence of RGL domain PF06045 was used to search RGL genes within the genomes of *F. × ananassa* (Camarosa Genome Assembly v1.0.a2; Liu et al., 2021), *F. vesca* (*Fragaria vesca* Whole Genome v4.0.a2; Li et al., 2019), and *F. iinumae* (Edger et al., 2020). The Blastp tool of the Genome Database for Rosaceae was employed (<https://www.rosaceae.org/>). The topology of protein sequences was analyzed with DeepTMHMM software (<https://biolib.com/DTU/DeepTMHMM/>).

Phylogenetic analysis of RGLyase proteins was conducted by the Maximum Likelihood method and JTT matrix-based model. The bootstrap consensus tree was inferred from 100 replicates. Branches corresponding to partitions reproduced in less than 50% of bootstrap replicates are collapsed. The tree was constructed using MEGA11 and displayed and annotated with iTOL v5.

### 2.3. Generation of transgenic strawberry plants

The binary vector pFNR-*FaRGLyase1*, containing a 475 bp non-conserved region of the *FaRGLyase1*, was used for genetic transformation. This vector was previously obtained by Molina-Hidalgo et al. (2013) and successfully used for RNAi silencing of the gene in transient transformation studies. The plasmid was introduced in *Agrobacterium tumefaciens* strain AGL1. Leaf disks from micropropagated strawberry plants were precultured for eight days in regeneration medium (micropropagation medium above described without kinetin and supplemented with 8.8  $\mu$ M benzylaminopurine (BAP) and 2.46  $\mu$ M indole-3-butyric acid (IBA) (Barceló et al., 1998). Then, explants were inoculated with a diluted culture of the *A. tumefaciens*, cocultured for two additional days in the same medium, and transferred to the selection medium (regeneration medium supplemented with 25 mg l<sup>-1</sup> kanamycin and 500 mg l<sup>-1</sup> carbenicillin). Regenerated shoots were micropropagated and rooted in the presence of 25 mg l<sup>-1</sup> kanamycin and acclimated to *ex vitro* conditions.

### 2.4. Phenotypic analysis of transgenic RGLyase1 plants

After acclimatization, primary transgenic plants from eleven independent lines were propagated by runners in the greenhouse, and daughter plants were used for phenotypic analysis. Non-transformed plants were used as controls. Fruits were collected from February to June at the stage of full ripeness, 100% red surface. Fruit color was measured with a colorimeter Minolta Chroma Meter CR-400. The L\*a\*b\* color space parameters (lightness, redness, yellowness) were recorded. Soluble solids were measured using a refractometer (Atago N1), and firmness using a hand-held penetrometer (Effegi) with a cylindrical needle of 9.62 mm<sup>2</sup> surface. Six to 10 plants per line were cultivated, and a minimum of 10 ripe fruits per line were assessed.

In a different experiment, the growth of fruits from control and selected transgenic lines was measured. Flowers at anthesis, with receptacles of about 5 mm, were tagged and photographed every three days until full ripening. The length of the longitudinal axis of the fruit at each sampling day was measured in the pictures using ImageJ. Data were fitted to a logistic growth curve, and relative growth rates were calculated (Paine et al., 2012). Eight to 10 flowers per genotype were tagged, and each point of the curve corresponds to a minimum of three independent fruits per genotype.

## 2.5. Molecular analysis of transgenic RGLyase1 plants

Total RNA was isolated from independent pools of de-achened ripe fruits, as reported by Gambino et al. (2008). The RNA obtained was treated with RNase-free DNase I (Roche) and purified through the RNeasy Mini-Elute Cleanup kit (Qiagen). RNA concentration and purity were evaluated using a Nanodrop™ spectrophotometer ND-1000 (Thermo Scientific) and 1% agarose gel electrophoresis. The gene expression analysis of *FaRGLyase1* and *FaMyb10* genes was performed by quantitative real-time PCR (qRT-PCR) through a CFX96 Touch Real-Time PCR Detection System. The *FaRGLyase1* gene primer sequences for quantitative amplification were 5'-TCCCTGATCGCTCAGCTGCCGA-3' and 5'-TCGTGAGAGTTGGATCCTC GTGCCG-3', and those for *FaMyb10* 5'-CGGCTTCATACGCAAAGCAA-3' and 5'-GAGTCTGTGGTGGTGTGTT-3'. The interspacer 26S–18S reference gene, which exhibits constitutive expression during fruit ripening, was used for normalization (Amil-Ruiz et al., 2013). Relative differential expression was determined by using the  $2^{-\Delta\Delta Ct}$  method (Pedersen and Amtssygehus, 2001).

For transcriptomic analysis, total RNA from control and transgenic ripe fruits from selected lines RG26 and RG87 was extracted as described previously. RNA quantity and integrity were checked by nanodrop, agarose gel electrophoresis, and Agilent 2100 bioanalyzer, with RNA integrity number (RIN) higher than 8 for all replicates. Three independent biological replicates were used. Libraries with insert sizes ranging from 150 bp to 200 bp were constructed and sequenced using an Illumina HiSeq 2000 at the Novogene Bioinformatics Institute, Beijing. More than 80 million reads per sample were generated. These sequences were mapped to the 'Camarosa' *F. × ananassa* Genome Assembly v1.0.a2 using TopHat2. The gene expression level was estimated by counting the reads that map to genes or exons and expressed as fragments per kilobase of transcript sequence per million base pairs sequenced (FPKM). For differential expression analysis, log2fold change values were calculated from normalized transgenic and wild-type read counts; a negative binomial distribution was used to estimate the associated probability, and those genes with an adjusted P-value <0.05 were considered as differentially expressed genes (DEGs).

## 2.6. Extraction and analysis of fruit cell walls

De-achened frozen fruits from control and selected transgenic lines at the stage of full ripeness were milled to powder under liquid nitrogen and extracted with PAW (phenol:acetic acid:water, 2:1:1, w/v/v) as described previously (Santiago-Doménech et al., 2008). Briefly, 10 g of fruit powder was extracted with 20 ml of PAW. After centrifugation at 4000g, pellets were de-starched by aqueous DMSO 90% treatment, and the final residue was lyophilized, considered the cell wall (CWM) extract. The CWM (150 mg) was sequentially extracted following the procedure of Santiago-Doménech et al. (2008) to obtain fractions enriched in pectins (water, CDTA, and sodium carbonate solubilized fractions) and hemicellulose (KOH 1M and KOH 4M). The carbazol method was used for measuring the uronic acid (UA) content in PAW and cell wall fractions, using GalA as the standard. The neutral sugar content was colorimetrically quantified following the orcinol method with glucose as the standard.

Comprehensive microarray polymer profiling (CoMPP) was performed using the protocol described in Kračun et al. (2017). For this analysis, high-throughput cell wall fractions were obtained by sequential homogenization of CWM with glass beads using a tissue lyser (Retsch MM400 mixer mill) for the following solvent series: sterile water; 0.1 M Na<sub>2</sub>CO<sub>3</sub>; 4 M KOH; and cadoxen [31% 1,2-diaminoethane with 0.78 M cadmium oxide (v/v)]. Both alkaline fractions included 0.1% NaBH<sub>4</sub> freshly added just before use. For the first water-soluble fraction, 10 mg of cell wall extract was homogenized in a tissue lyser with 500 µl of water at 30 Hz shaking for 20 min, followed by gentle rocking for 1 h at room temperature. After centrifugation at 2700g for 15 min, supernatants were saved in a fresh tube and stored as the water fraction, while

pellets were further extracted with the next solvent, following the same extraction steps. Supernatants of each fraction were diluted four times (first dilution 1:1 and 5-fold for the following dilutions) and printed as four technical replicates. All transgenic and wild-type samples were printed simultaneously on the same sheet of nitrocellulose as adjacent arrays using an ArrayJet Sprint (ArrayJet, Roslin, UK) and quantified as previously described (Kračun et al., 2017). The printed nitrocellulose sheets were probed with the primary monoclonal antibodies (mAbs) diluted (1/10) in phosphate-buffered saline (PBS) containing 5% (w/v) milk powder (MPBS). Secondary anti-rat or anti-mouse antibodies conjugated to alkaline phosphatase (Sigma) were diluted (1/5000) in MPBS. Primary mAbs used in this study (Supplementary Table 1) were obtained from the University of Leeds, UK, except RU1 and RU2, which were kindly provided by M.C. Ralet (Biopolymères Interactions Assemblages, Nantes, France). Developed microarrays were scanned (CanoScan 8800F), converted to TIFFs, and signals were processed by ImaGene 6.0 microarray analysis software (BioDiscovery). The mean spot signals obtained from four experiments are presented in heat maps in which color intensity was correlated to the signal. The highest signal in each dataset was set to 100, and all other values were normalized accordingly. A cut-off value of 5 was applied.

## 2.7. Immunolabelling of fruit sections

Small fruit cylinders, including cortical and pith tissues, were obtained from ripe fruits of control and transgenic plants. Samples were immediately fixed in a solution containing 4% (w/v) formaldehyde in PEM buffer (50 mM PIPES, 5 mM EGTA, and 5 mM magnesium sulfate; pH 6.9), subjected to a mild vacuum for 1 min, and incubated at 4 °C for 8 h. This procedure was repeated twice. The fixed samples were dehydrated in an ethanol series and infiltrated with resin LR White (Agar Scientific). Embedded samples were maintained at 50 °C for 24 h for resin polymerization. Thin sections (4 µm) were cut using a hard tissue microtome (Leica EM UC7) and mounted on silanized glass slides. Sections were processed for immunohistological analysis using RU1, LM5, and LM6-M mAb against RGI backbone, galactan, and arabinan lateral side chains, respectively. Briefly, the sections were blocked in PBS (0.1 M phosphate-buffered saline, pH 7.3; 0.3 M NaCl) with 5% milk powder for 30 min. After several washes with PBS, the sections were incubated with a primary antibody in a blocking buffer for 90 min, rinsed with PBS, and then incubated with a secondary antibody in a blocking buffer for 1 h. The secondary antibodies used were Goat anti-rat IgG conjugated with FITC (Sigma; 1:100 dilution) in the case of LM5 and LM6-M and Goat anti-mouse IgG conjugated with FITC (Sigma; 1:50 dilution) for RU1 mAb. The sections were rinsed with PBS three times and then stained with calcofluor (0.25 mg l<sup>-1</sup> in PBS) for 5 min. The control sections for the immunoassay were subjected to the same treatment, excluding the primary antibody incubation. The sections were mounted with Mowiol, and the green fluorescence was examined using a fluorescein isothiocyanate (FITC) filter block in an epifluorescence microscope (Nikon Eclipse E800). A minimum of five independent fruits per genotype were processed.

## 2.8. Statistical analysis

Data were subjected to ANOVA using R. Bartlett test for homogeneity of variance was performed prior to ANOVA. Tukey and Dunn tests were used for mean separation for homogeneous and non-homogeneous variances, respectively. All tests were performed at P = 0.05.

## 3. Results

### 3.1. Identification of RGLyase genes in *Fragaria*

Genes with homology to Pfam06045 domain, characteristics of RGLs proteins, were searched in the Genome Database for Rosaceae (GDR;

<https://www.rosaceae.org/>) using the *F. × ananassa* Camarosa Genome Assembly v1.0.a2 (Supplementary Table 2). Seventeen out of the 28 genes identified encoded proteins that displayed the typical arrangement of the three domains, RGL (PF06045), fn3 (PF14686), and CBM (PF14683), present in RGLs (McDonough et al., 2004). Protein length ranged from 638 to 722 aas (Supplementary Table 3). Three additional genes showed a complex structure encoding larger proteins (981–1431 aas) containing two sets of the three RGLs domains (FxaC\_2g26140.t1) or one or two additional Glycosyl hydrolase family 28 C-terminal domains (FxaC\_2g08540.t1; FxaC\_4g36680.t1). Finally, eight genes encode shorter proteins with incomplete domains or lacking fn3 and CBM domains. Only the 20 proteins containing the three RGL domains were used for further analysis. Sequence analysis by DeepTMHMM predicts that all these proteins were outside the cell, and 15 contained a signal peptide. Interestingly, FxaC\_2g26140.t1, encoding the larger RG

protein, displayed two transmembrane regions (Supplementary Table 3). *FaRGLyase1* protein sequence (Molina Hidalgo et al., 2013) corresponded to FxaC\_3g03480.

*RGLyase* genes were also searched in the genomes of *F. vesca* and *F. iinumae*, the diploid progenitors of cultivated strawberry (Feng et al., 2021) (Supplementary Table 4). In *F. vesca*, 12 *RGLyase* genes were found. The *F. vesca* genome used in the analysis included alternative splicing, and the *RGLyase* genes encoded 19 predicted proteins containing the complete set of RGLyase domains. The search in *F. iinumae* reported eight genes that encoded RGLyase proteins containing the three typical domains, two short sequences lacking one or two domains, and a large sequence with two sets of the three RGLyase domains.

A phylogenetic tree was built using the predicted strawberry RGL proteins containing the three functional domains and the eudicots RGLs previously analyzed by Mokshina et al. (2019). The *F. chiloensis* RGL

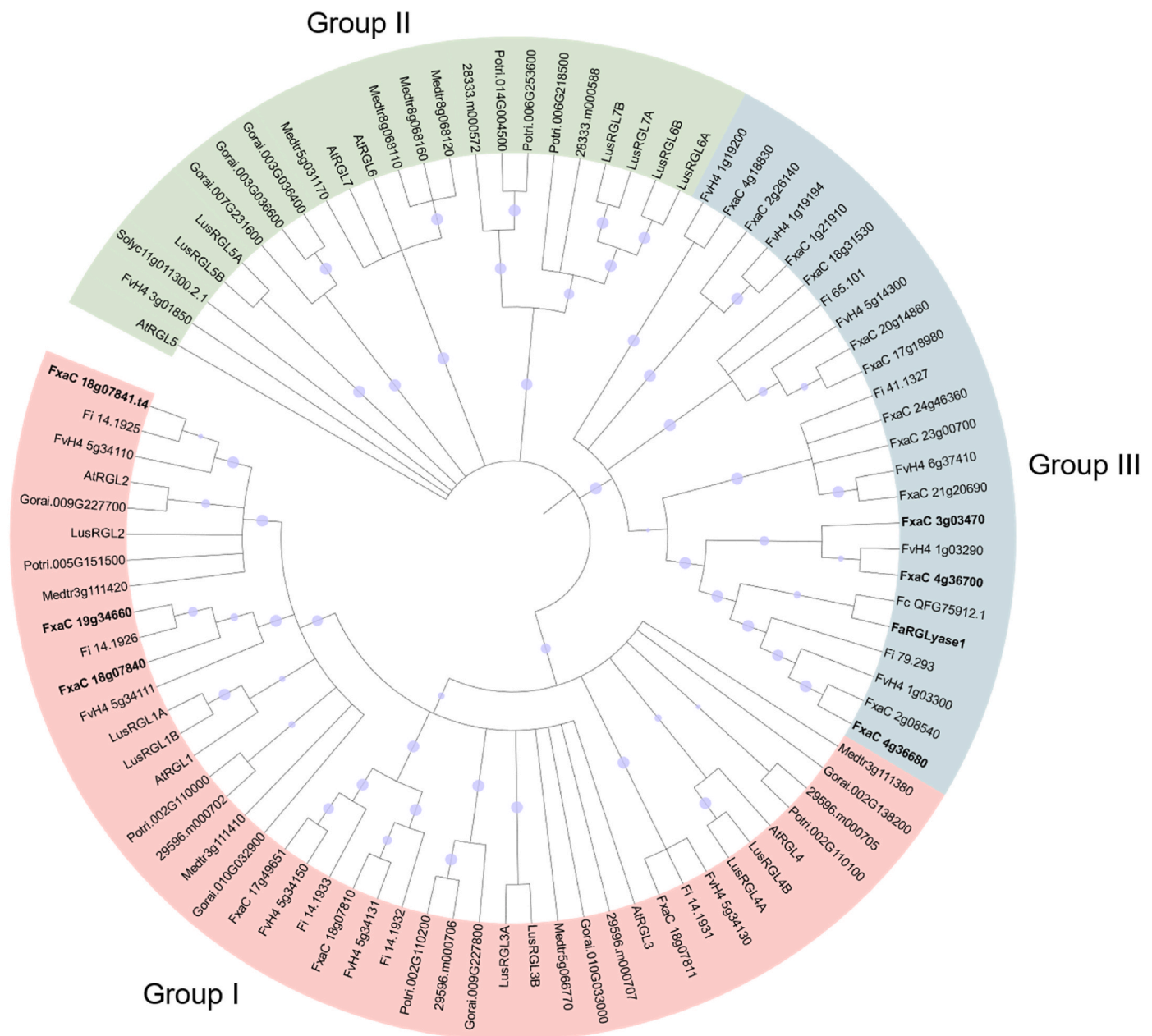


**Fig. 1.** Phylogenetic analysis of RGL proteins. The evolutionary history was inferred by using the Maximum Likelihood method and JTT matrix-based model, with 100 bootstraps. Branches corresponding to partitions reproduced in less than 70% bootstrap replicates are collapsed. Size of blue circles indicates bootstrap support of branches, in the range 70–100%. Evolutionary analyses were conducted in MEGA11 and the tree was displayed and annotated with iTOL v5. Genes used in the analysis are listed in Supplementary Table 5. *Fragaria × ananassa* genes in bold correspond to those expressed in fruit.

gene *FchRGL1* (FcQFG75912.1) described by Méndez-Yañez et al. (2020) and the *Solanum lycopersicum* RGL gene Solyc11g011300 (Ochoa-Jiménez et al., 2018) were also included in the analysis (Fig. 1). Mokshina et al. (2019) found that RGLs from several dicot species were separated into two clades, namely Group I and II. In the present study, proteins from Group I also appeared grouped into the same Clade (named Group I in this research, following the nomenclature of Mokshina et al. (2019)). However, RGLs from Group II formed a heterogeneous group that was actually separated into different species-specific clades. Some strawberry RGLs were included in Group I, which was the most numerous. However, most of the *Fragaria* proteins formed a separate clade, Group III. On the other hand, all *F. × ananassa* genes appeared closely clustered with their corresponding *F. vesca* or *F. iinumae* homolog genes. Finally, *F. chiloensis FchRGL1* displayed a high identity level with *FaRGLyase1* protein in Group III.

A transcriptome study by RNAseq in cv. ‘Chandler’ fruits showed that only five RGL genes were expressed in the red receptacle. The expression level of *FaRGLyase1* was significantly higher than the other RGLs (Fig. 2). Similarly, the analysis of the transcriptomic data reported by Liu et al. (2021) showed the expression of four RGL genes during ‘Camarosa’ fruit development (Supplementary Fig. 1). The expression of three out of four of these genes, including *FaRGLyase1*, was induced during fruit ripening. However, in ‘Camarosa’ fruits, the highest expression level corresponded to Fxa\_4g36680.

### 3.2. Generation and characterization of RNAi transgenic lines

Leaf explants from micropropagated ‘Chandler’ plants were transformed with *A. tumefaciens* harboring the RNAi sequence from *FaRGLyase1* described in Molina-Hidalgo et al. (2013). Eleven independent transgenic lines showing active growth in the presence of kanamycin were obtained. These plants were acclimated to greenhouse conditions for molecular and phenotypical evaluation. No vegetative alterations were observed in the transgenic lines, with the growth pattern similar to control plants. The *FaRGLyase1* expression level was measured in whole ripe fruits. Nine out of the 11 lines obtained showed a significant down-regulation of the gene, higher than 90% (Fig. 3). The expression level of *FaMyb10*, a master regulator of anthocyanin biosynthesis, was

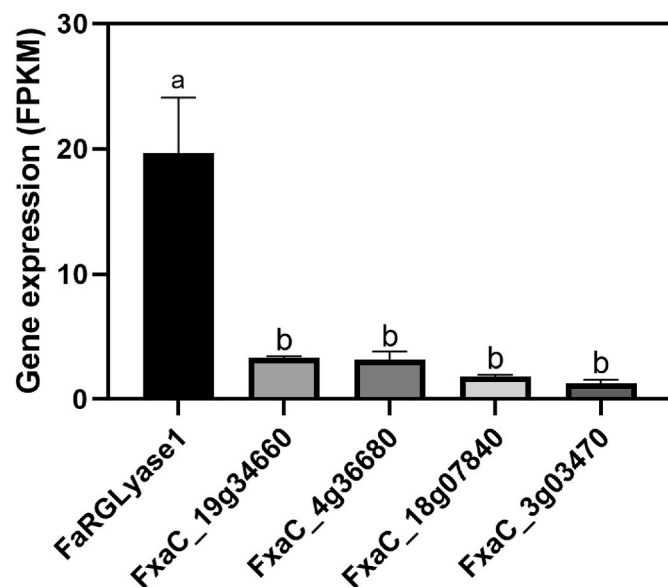


Fig. 2. Expression of RGL genes in ripe strawberry, cv. ‘Chandler’. Gene expression values were obtained in an RNA-seq study performed in ripe receptacles and correspond to fragments per kilobase of transcript sequence per million base pairs sequenced (FPKM). Columns with different letters indicate significant differences by Tukey test at  $P = 0.05$ .

also measured in the same samples as a marker of the fruit ripening stage. All fruits displayed similar or even higher *FaMyb10* mRNA levels than wild type fruits (Supplementary Fig. 2).

Fruit weight, size, and soluble solid content in wild type and transgenic ripe fruits are shown in Table 1. In general, fruit weight was slightly lower in the transgenic lines, although the differences with wild type fruits were not significant. Fruit length was significantly reduced in RG1, RG52, and RG54, while fruit width was not significantly affected. Similarly, *FaRGLyase1* silencing did not modify soluble solids content. Regarding fruit firmness, fruits from lines RG26, RG84, and RG87 were significantly firmer than wild type (Fig. 4). Mean values of fruit firmness in the different lines were negatively correlated with *FaRGLyase1* gene expression level (Pearson correlation coefficient of  $-0.73$ , significant at  $P = 0.05$ ).

Transgenic lines RG26 and RG87 were selected for further studies. The phenotypic analysis of these lines was performed in daughter plants obtained by runner propagation. Flowers from control and transgenic lines were tagged at anthesis, and fruit length was measured until ripening to determine fruit growth rates. Images of control and transgenic fruits at different developmental stages are shown in Supplementary Fig. 3. Fruit length data were adjusted to a logistic growth curve, obtaining  $R^2$  values higher than 0.97 (Supplementary Fig. 4). The parameters of the logistic curves were not statistically different in control and transgenic lines. Relative growth rates (RGR) calculated from the logistic curves were slightly higher in the transgenic lines during the initial developmental phases until day 20 but lower than the control at the final ripening stages (Supplementary Fig. 4). Most fruits reached the commercial mature stage, more than 80% of the fruit surface red, 28–30 days after anthesis, independently of the genotype. Fruit quality parameters were measured at full ripeness. The results obtained were similar to those previously described (Table 2). Fruits from RG26 lines were slightly smaller than wild type, but neither soluble solids content nor fruit color were affected (Table 2). Both transgenic lines produced fruits significantly firmer than the control, ranging the increment in firmness from 15% in RG87 to 32% in RG26.

### 3.3. Cell wall analysis of transgenic fruits

Cell walls were extracted from ripe receptacles of wild type and selected transgenic lines using PAW (phenol:acetic acid:water) to inactivate cell wall enzymes. The yield of cell wall material (CWM) was similar in control and transgenic lines, ca. 0.9 g CWM/100 g FW; however, the amount of PAW soluble fraction was significantly higher in the transgenic lines,  $0.30 \pm 0.03$  g PAW/100 g FW in WT vs.  $0.43 \pm 0.03$

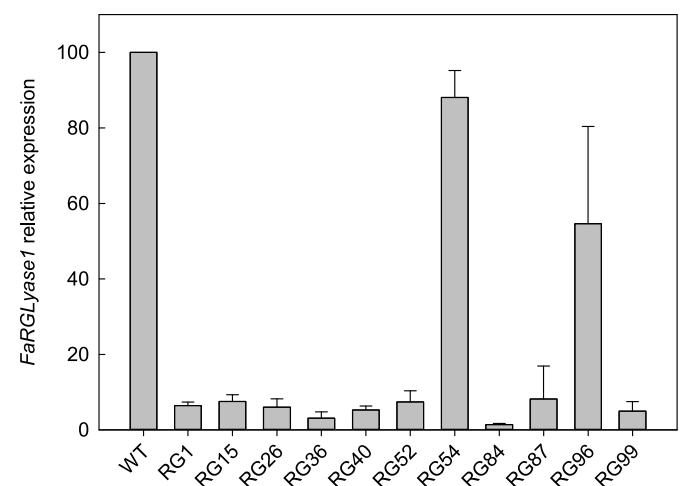
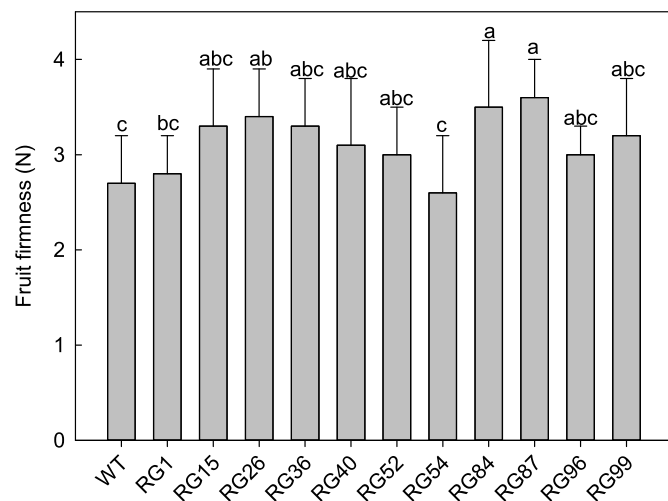


Fig. 3. *FaRGLyase1* gene expression in ripe fruits from transgenic RNAi lines measured by qRT-PCR. Expression levels were normalized to the wild type (WT). Data correspond to mean  $\pm$  SD of three biological replicates.

**Table 1**

Characteristics of ripe fruit in wild type and transgenic *FaRGLyase1* RNAi lines. Data represent mean ± SD of a minimum of 10 fruits per line. Mean separation by Tukey (weight, length and width) or Dunn (soluble solids) tests at P = 0.05.

Line	Weight (g)	Length (cm)	Width (cm)	Soluble solids
WT	9.0 ± 2.9 ab	2.2 ± 0.4 ab	1.4 ± 0.3 ab	8.6 ± 1.8 ab
RG1	6.3 ± 1.7 b	1.6 ± 0.3 cd	1.1 ± 0.3 b	8.6 ± 2.1 ab
RG15	9.4 ± 3.1 ab	2.0 ± 0.5 abc	1.5 ± 0.4 ab	9.1 ± 2.6 ab
RG26	7.4 ± 3.1 ab	1.7 ± 0.5 bcd	1.4 ± 0.4 ab	9.1 ± 2.4 ab
RG36	6.9 ± 2.6 b	1.8 ± 0.5 bcd	1.2 ± 0.4 ab	11.4 ± 3.2 a
RG40	8.0 ± 2.6 ab	1.9 ± 0.5 abcd	1.2 ± 0.4 b	8.3 ± 1.8 ab
RG52	6.2 ± 2.7 b	1.4 ± 0.5 d	1.2 ± 0.3 ab	11.2 ± 2.8 a
RG54	6.2 ± 1.5 b	1.4 ± 0.3 d	1.1 ± 0.3 b	10.7 ± 2.4 ab
RG84	7.2 ± 1.8 ab	1.7 ± 0.3 bcd	1.2 ± 0.2 b	9.6 ± 2.8 ab
RG87	8.3 ± 2.5 ab	1.8 ± 0.5 bcd	1.2 ± 0.3 ab	10.7 ± 3.3 ab
RG96	10.3 ± 3.5 a	2.4 ± 0.6 a	1.6 ± 0.4 a	8.0 ± 1.1 b
RG99	7.9 ± 2.8 ab	1.9 ± 0.5 abcd	1.3 ± 0.3 ab	8.9 ± 1.7 ab



**Fig. 4.** Firmness in ripe fruits from wild type and transgenic *FaRGLyase1* RNAi lines. Data correspond to mean ± SD of a minimum of 10 fruits per line. Mean separation by Tukey test at P = 0.05.

and 0.40 ± 0.01 in RG26 and RG87 transgenic lines, respectively. CWM was extracted with different solvents to obtain fractions enriched in water-soluble, ionically bound- and covalently bound-pectins (water, CDTA, and Na<sub>2</sub>CO<sub>3</sub> fractions, respectively) and hemicellulosic polymers (KOH 1M and 4M fractions). The amount of pectin-enriched fractions was higher in transgenic fruits. In contrast, yield of hemicellulosic material was not altered (Fig. 5A). Pectin content was measured in the different pectin fractions and in the hemicellulosic fractions (Fig. 5B). A significantly higher amount of UA was observed in water and CDTA fractions from both transgenic lines when compared with wild type fruits; by contrast, Na<sub>2</sub>CO<sub>3</sub> contained similar UA contents. As expected, the pectin contents in both hemicellulosic KOH fractions were lower than those observed in the pectin fractions, and there were no statistical differences in transgenic and wild type fruits. The total amount of UA in the different cell wall fractions analyzed increased by 34% as a result of *FaRGLyase1* down-regulation, 14.9 mg.100 mg<sup>-1</sup> CWM in WT vs. 20.5

**Table 2**

Characteristics of ripe fruit in wild type and selected transgenic *FaRGLyase1* RNAi lines RG26 and RG87. Data represent means ± SD of a minimum of 10 fruits per line. Mean separation by Tukey (color and SS) or Dunn (weight, length, width and firmness) tests at P = 0.05.

	Weight (g)	Length (cm)	Width (cm)	Soluble solids	Firmness (N)	Color		
						L	a*	b*
WT	10.0 ± 3.9a	3.3 ± 0.5a	2.3 ± 0.4a	8.2 ± 2.5a	3.4 ± 0.8b	35.7 ± 3.9 ab	36.3 ± 3.8a	33.1 ± 11.7a
RG26	8.2 ± 2.6b	2.7 ± 0.4b	2.2 ± 0.3a	8.1 ± 2.5a	4.5 ± 0.9a	38.0 ± 0.5a	34.2 ± 5.8a	35.4 ± 9.6a
RG87	11.2 ± 4.0a	3.4 ± 0.5a	2.3 ± 0.4a	7.3 ± 1.9a	3.9 ± 0.9a	34.9 ± 4.0b	35.8 ± 4.4a	29.5 ± 12.2a

and 19.4 mg.100 mg<sup>-1</sup> CWM in RG26 and RG87 transgenic lines, respectively. Neutral sugar content was also higher in all fractions from transgenic fruits when compared with control; however, the differences were only significant in CDTA and KOH 1M fractions (Supplementary Fig. 5).

Fractions rich in loosely and tightly bound pectins (water and Na<sub>2</sub>CO<sub>3</sub> fractions, respectively), xyloglucans (KOH 4M), and matrix polysaccharides highly imbricated into cellulose microfibrils (cadoxen) were subjected to Comprehensive Microarray Polymer Profiling (CoMPP) using a set of mAbs against different cell wall epitopes (Supplementary Table 1). A heatmap showing the relative abundance of the glycans recognized by the mAbs is shown in Fig. 6. The abundance of RGI epitopes, both RGI backbone, recognized by RU1 and RU2, and galactan (LM5) and arabinan (LM6-M) side chains was higher in water, sodium carbonate and cadoxen fractions of the transgenic lines. The increase in RGI epitopes was also observed in the KOH fractions of transgenic lines, although the differences with the control were lower. LM13 against linearized arabinan and LM26 against branched galactan only yielded a weak signal in KOH and cadoxen fractions; as observed for the backbone and side chains mAbs previously mentioned, the

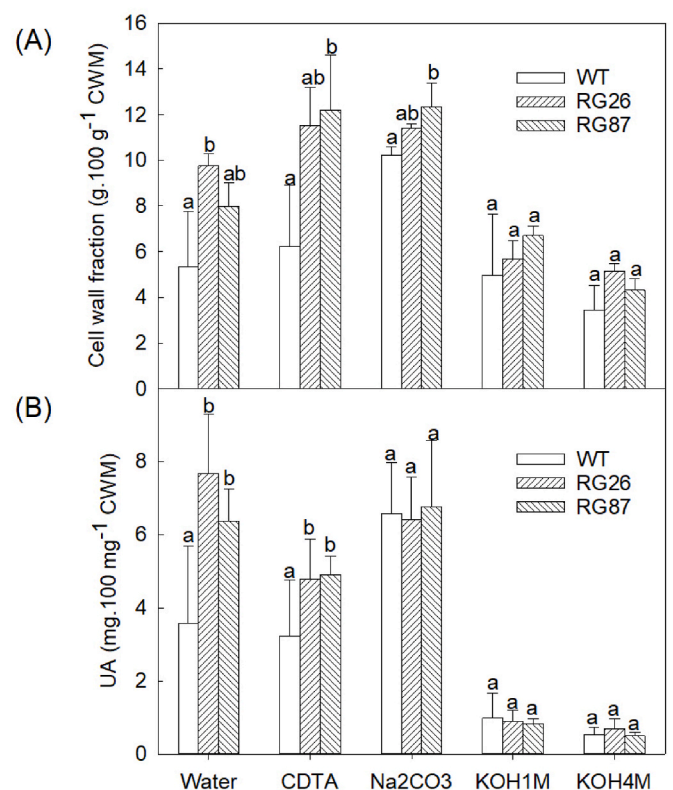


**Fig. 5.** Cell wall analysis in control (WT) and transgenic *RGLyase1* RNAi lines. CWM was sequentially extracted with water, CDTA, Na<sub>2</sub>CO<sub>3</sub>, and KOH 1M and 4M, and the weight (A) and uronic acid content (B) in the different cell wall fractions were measured. Bars represent mean ± SD. Within each fraction, bars with different letters indicate significant differences by Tukey test at P = 0.05.

signals of LM13 and LM26 were higher in transgenic lines. Silencing of the *RGLyase1* gene also increased the low methyl-esterified HG pectins detected with LM18 and LM19 mAbs in Na<sub>2</sub>CO<sub>3</sub>, KOH, and cadoxen fractions from transgenic lines. Interestingly, in the water fraction, the abundance of methyl-esterified HG pectins recognized by JIM7 was significantly higher in the transgenic lines than in the control. Regarding cross-linking glycans, the abundance of xyloglucan epitopes (LM15 and LM25) was similar in control and transgenic lines; by contrast, mAbs directed to xylans, especially LM28, showed a stronger signal in control fruits. Finally, the abundance of arabinogalactan-protein epitopes, recognized with JIM13, was higher in transgenic lines in all fractions analyzed.

The higher abundance of RGI in transgenic cell walls was confirmed by immunohistochemical analysis of ripe fruit sections. The RU1 mAb against RGI backbone yielded stronger signals in transgenic lines when compared with wild type (Fig. 7) in both vascular bundles and parenchyma cells. The signal was restricted to the cell walls and it did not appear in the middle lamella. LM5 also showed a slightly stronger signal in transgenic fruits, denoting a higher amount of RGI-galactan side chains (Supplementary Fig. 6); however, no apparent differences between transgenic and wild type were detected with LM6-M against arabinan side chains (Supplementary Fig. 6).

### 3.4. Transcriptomic analysis of transgenic fruits

An RNA-seq analysis was performed using RNA extracted from the red receptacle of wild type and RG26 and RG87 transgenic fruits to determine transcriptomic changes. On average, 86,769,830 clean reads per sample were obtained, and they were mapped to the ‘Camarosa’ *F. × ananassa* Genome Assembly v1.0.a2. A total of 550 DEGs relative to the wild type, 166 down-regulated and 384 up-regulated, were obtained in the line RG26. The number of DEGs was lower in RG87 fruits; 190 genes were differentially expressed compared to control, 106 down-regulated and 84 up-regulated. Among all these genes, 67 DEGs, 38 down-regulated and 29 up-regulated, were shared in both transgenic lines, representing 12% and 34% of all DEGs found in RG26 and RG87 transgenic lines, respectively. The complete list of common DEGs is shown in Supplementary Table 6. Besides *FaRGLyase1*, other genes involved in cell wall remodeling were down-regulated. These genes

included two additional RGLs, FxaC\_3g03470.t1 and FxaC\_4g36680.t1, and two xyloglucan endotransglucosylase/hydrolases. A Trichome birefringence-like 39 gene, involved in secondary cell wall deposition, was also down-regulated. Additionally, *FaRGLyase1* suppression induced the down-regulation of other genes related to heavy metal detoxification and oxidative stress (several metallothionein genes), metal ion transport (ZRT/IRT-like protein), protein hydrolysis (Cysteine and Zn-dependent peptidases), lipid hydrolysis and transfer (several GDSL-like lipases and a lipid-transfer protein), fatty acid biosynthesis (3-ketoacyl-CoA synthase 10), programmed cell death (legumain), protein modifications and secondary metabolism (methyl and acyl transferases), stress response (heat shock protein, RNA binding), auxin signaling (auxin canalization protein DUF828), and two tRNA synthases.

The up-regulated DEGs common to both transgenic lines that could be involved in cell wall metabolism included a β-xylosidase protein and a SKU5 monocopper oxidase-like protein; this last one has been implicated in cell wall synthesis in Arabidopsis roots (Zhou, 2019). Several metal ion homeostasis genes were also up-regulated (a Zn-binding protein and two ferretins), as well as a large number of genes involved in many diverse physiological processes, such as development and stress adaptation (regulator of nonsense transcript protein, concanavalin A-like lectin protein kinase, pathogenesis-related protein 1), cell division (GTP-binding protein 15), transport of vesicles (syntaxin of plants 124), protease inhibitor (serine protease inhibitor), ion transport and pH regulation (alpha carbonic anhydrase, blue-copper-binding protein), protein modifications and secondary metabolism (acyl and methyl transferases), auxin metabolism (indole-3-acetate beta-D-glucosyltransferase), transcription factors (WRKY DNA-binding protein 15, putative transcription factor/chromatin remodeling BED-type(Zn) family).

## 4. Discussion

Studies on cell wall remodeling process during fruit softening have mainly been focused on the role of enzymes degrading HG (e.g. polygalacturonase, pectate lyase, pectin methyl esterase), neutral side chains of RGI (galactosidase, arabinase), and xyloglucan/cellulose degrading enzymes (xyloglucan endotransglucosylase/hydrolase, endoglucanases) (Wang et al., 2018). RGLyases cleave the backbone of RGI internally. Despite this polysaccharide being a principal component of the primary cell wall, the function of RGLyases during fruit softening has received little attention. In this study, we show evidence that RGLyases participate actively in the disassembly of the cell wall during strawberry fruit softening. However, its impact on fruit texture is modest compared to the effect of HG degrading enzymes.

### 4.1. RGLyases constitute a small gene family in *Fragaria*

RGLyases found in plants belong to the PL4 family and contain three functional domains, i.e., a catalytic domain and two domains presumably involved in binding to the polysaccharide substrate (Morales-Quintana et al., 2022). The blast search of the catalytic domain in the genome of *F. × ananassa* and their putative progenitors, *F. vesca* and *F. iinumae*, reported a small gene family comprised of 20, 12 and 8 genes, respectively, putatively encoding functional proteins with the three RGL domains. Similarly, the number of predicted RGL genes in other species was relatively low, e.g., 7 genes in Arabidopsis (Mokshina et al., 2019), 13 genes in tomato (Berumen-Varela et al., 2017). The reduced size of the RGL gene family contrasts with other genes encoding cell wall pectinases. For instance, 82 sequences are annotated as PG genes in *F. vesca* (Paniagua et al., 2020), and 65 pectate lyase and 54 PME have been reported in *F. × ananassa* (Xue et al., 2020; Lin et al., 2023). Mokshina et al. (2019) clustered eudicots RGLs in groups I and II. When the *Fragaria* RGL genes found in this research were included in the phylogenetic analysis, these sequences were distributed in group I and in a new cluster, group III, formed exclusively by *Fragaria* genes. Among the 20 RGL genes found in *F. × ananassa*, only five were expressed in ‘Chandler’ ripe fruits, corresponding the higher

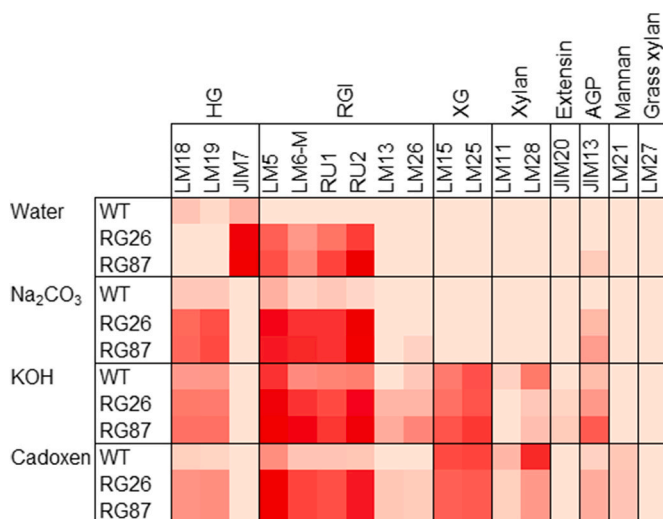
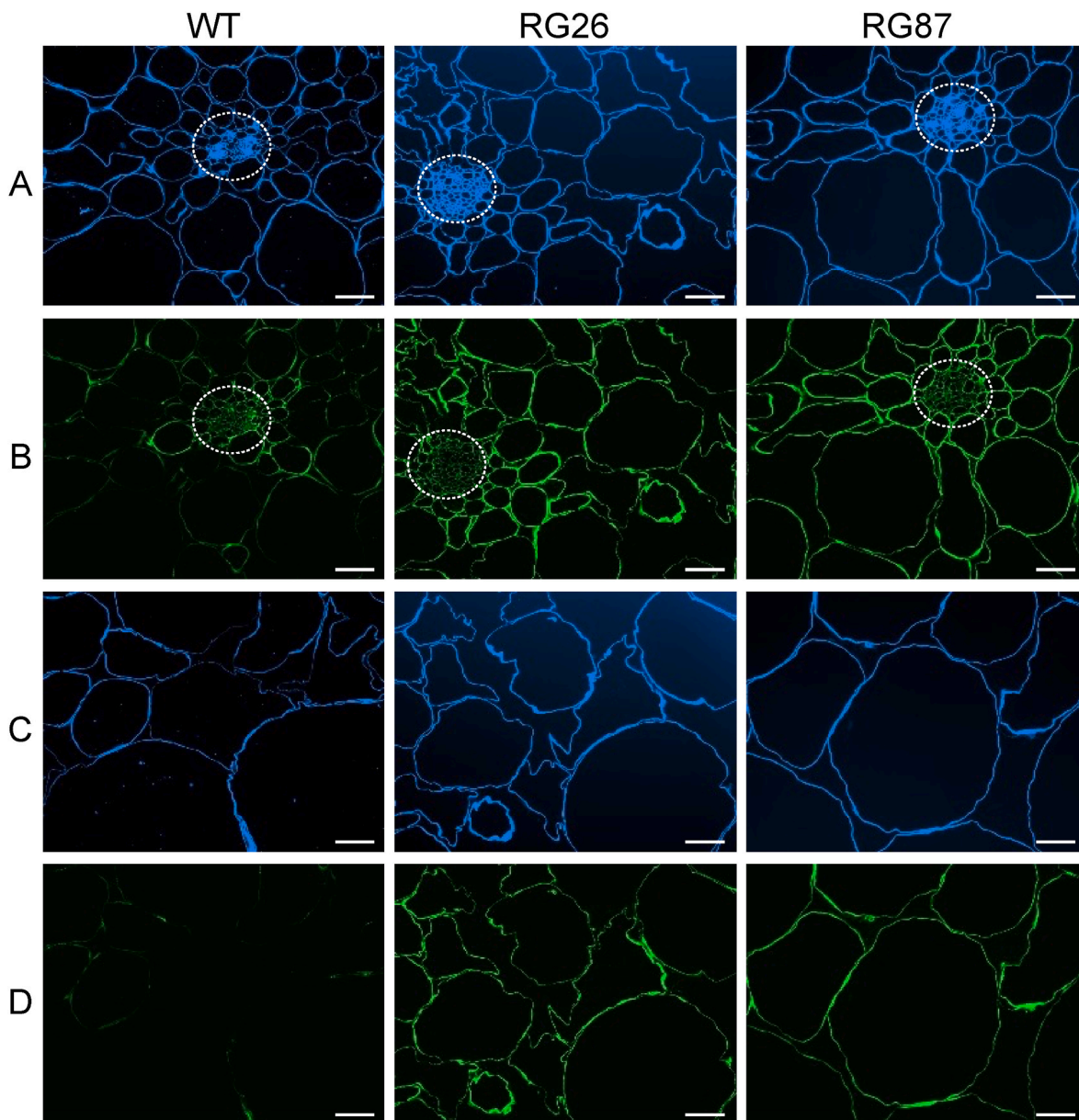


Fig. 6. Heat map showing the relative abundance of cell wall epitopes recognized by various mAbs in cell wall fractions extracted from ripe strawberry fruits of control (WT) and *RGLyase1* RNAi lines. A value of 100 was assigned to the highest mean spot signal and all other signals were adjusted accordingly. The LM27 mAb specific against grass xylan was used as negative control. HG, homogalacturonan; RGI, rhamnogalacturonan I; XG, xyloglucan; AGP, arabinogalactan proteins.



**Fig. 7.** Immunolabelling of RGI pectin domains in cell walls from ripe fruits of control (WT) and transgenic *FaRGLyase1* selected lines RG26 and RG87. Tissue sections proximal (A, B) or distal (C, D) to a vascular bundle were stained with calcofluor (A, C) or incubated with RU1 monoclonal antibody (B, D) specific against RGI backbone. Vascular bundle regions are surrounded by dashed white circles. Scale bars: 25  $\mu\text{m}$  (A, B), 50  $\mu\text{m}$  (C, D).

expression level to *FaRGLyase1*. This gene was included in Group III and was clustered with *FchRGL1*, which has been involved in the softening of *F. chiloensis* fruits (Méndez-Yañez et al., 2020).

#### 4.2. *FaRGLyase1* down-regulation has a limited effect on strawberry fruit softening

Most transgenic lines expressing the *FaRGLyase1* RNAi construct displayed a significant reduction in the *FaRGLyase1* mRNA levels in ripe fruits. However, fruit firmness increased significantly only in three out of the eleven transgenic lines obtained. The highest increase in firmness achieved was 32% relative to wild type fruits, observed in line RG26. Previous studies characterized the effect of other genes encoding cell wall pectinases in transgenic strawberry using the same genotype, cv. 'Chandler', employed in this research. The silencing of *Fa $\beta$ Gal4*, encoding a  $\beta$ -galactosidase, yielded a similar increase in fruit firmness to the one achieved with *FaRGLyase1* (Paniagua et al., 2016). This class of

enzymes also acts on RGI, removing galactose units from lateral side chains. It is thought that this process contributes to the solubilization of pectins during fruit ripening (Brummell, 2006; Paniagua et al., 2016). The suppression of HG depolymerization by the genetic manipulation of the levels of PG genes through antisense silencing (Paniagua et al., 2020) or gene editing (López-Casado et al., 2023) yielded higher increases in firmness of ripe strawberry fruits, reaching up to 70%. Similar values were also obtained in antisense pectate lyase *Fap1C* plants (Jiménez-Bermúdez et al., 2002), an enzyme that depolymerizes demethylated HG by a  $\beta$ -elimination reaction. Together, these results suggest that the disassembly of HG during fruit ripening has a higher impact on fruit softening than the remodeling of RGI pectin domains.

#### 4.3. Remodeling of RGI but also HG is impaired in *FaRGLyase1* RNAi fruits

Solubilization of pectins tightly bound to the cell wall matrix generally

occurs during the softening of many fleshy fruits, including strawberry (Brummell, 2006). This process mainly occurs in this fruit at the expense of pectins extracted with CDTA and sodium carbonate (Paniagua et al., 2017a). Although the ultimate reasons for this process are unclear, it is thought that the depolymerization of HG and xyloglucans and the loss of arabinan and galactan side chains are the leading causes (Brummell et al., 2022). At the cell wall level, transgenic *FaRGLyase1* fruits displayed a higher amount of pectins, especially in water and CDTA fractions. However, the amount of sodium carbonate polyuronides remained similar to the control. Fruits with the *FaPG1* gene down-regulated also showed reduced pectin solubilization (Paniagua et al., 2020); however, in that case, both CDTA and sodium carbonate fractions were enriched in pectins when compared with controls. The minor effect of *FaRGLyase1* silencing on sodium carbonate pectin fraction might be due to a lower RGI abundance in pectins tightly bound to the cell wall.

The preservation of RGI from extensive degradation in transgenic fruits was observed in the immunohistological sections and in the carbohydrate microarray of *FaRGLyase1* fruits. Tissue sections labeled with antibodies against the RGI backbone showed a higher signal in transgenic fruit than controls. Similarly, in the polysaccharide profile, the abundance of RGI epitopes was higher in both transgenic lines when compared with the control in the four cell wall fractions analyzed. Interestingly, a large amount of RGI backbone and galactan and arabinan sidechain epitopes were detected in the KOH and the cadoxen fractions, cell wall extractions targeting xyloglucan and cellulose microfibrils, respectively. In the most accepted cell wall model, pectins and cellulose/hemicellulose are depicted as separated networks from each other (Kaczmarek et al., 2022). However, previous pieces of evidence suggest that RGI could be linked to or entrapped in the cellulose microfibrils. In *Arabidopsis* cell walls, around 25–50% of surface cellulose binds pectins, while the cellulose–xyloglucan contacts are more limited than previously thought (Wang and Hong, 2016). The nature of the linkages involved in binding pectins to cellulose is unclear. Zykwincka et al. (2006) suggested that both polysaccharides could be covalently and non-covalently bound. According to Höfte and Voxeur (2017), this process occurs mainly through xylans but also, with a lower affinity through arabinan and galactan side chains of RGI. Interestingly, the relative abundance of heteroxylan epitopes, mAb LM11 and LM28, was lower in the transgenic lines than in control. On the other hand, transgenic lines displayed higher signals of JIM13 against arabinogalactan-proteins being especially abundant in KOH fraction, confirming that RGI could also be linked to AGP, as Tan et al. (2013) suggested. Notably, most changes detected in the cell walls of *FaRGLyase1* described above were similar to those observed in antisense PG fruits (Paniagua et al., 2020). Significant amounts of HG, but also RGI, were detected in the xyloglucan–cellulose fraction due to silencing of PG genes in strawberry fruit. Pectin structural organization *in muro* is far from clear. The most accepted hypothesis suggests that sections of HG are interspersed with blocks of RGI, creating a complex polysaccharide with alternating smooth and hairy regions (De Vries et al., 1982). According to this model, it would be expected that the restriction of RGI degradation exerted a minor effect on HG abundance (*FaRGLyase1* transgenic fruits) or vice versa (*FaPG* downregulated fruits; Paniagua et al. (2020)). On the contrary, the results found in these transgenic fruits suggest that both pectin domains could be more tightly linked, or maybe the HG and RGI domains have an interspersed pattern that favors the degradation of one to have a greater effect on the other. Other alternative pectin structural models could explain these results. Vincken et al. (2003) proposed that HG and xylogalacturonans are side chains of an RGI backbone. Yapo (2011) and Paniagua et al. (2017b) depicted similar models in which pectins in the cell wall would be formed by an RGI core decorated by short HG chains. On the other hand, our results also indicate that the cellulose/hemicellulose network could also be a source of soluble pectins during strawberry softening, so instead of independent networks, our results support the potential connection among all the polymers in the wall.

#### 4.4. Transcriptomic changes in *FaRGLyase1* ripe fruits

Previous studies showed that the transgenic modification of genes encoding cell wall proteins can affect the expression of unrelated genes involved in cell wall remodeling. For instance, suppressing the expansin *LeExp1* in tomato reduced PG gene expression (Brummell et al., 2022). Many cell wall-related genes were down-regulated in transgenic strawberry fruits expressing antisense sequences of PG genes, including several PME,  $\beta$ -Galactosidases, and endo-glucanases (Paniagua et al., 2020). These results indicate that a complex network of unknown feedback regulation exists in the cell wall, perhaps related to the action of oligosaccharins released during fruit ripening. The silencing of *FaRGLyase1* modified the expression of a few numbers of genes encoding cell wall proteins. Notably, two XTH genes were down-regulated while a  $\beta$ -Xylosidase was upregulated. XTHs catalyze the cleavage of xyloglucans, generating reducing ends, and their linking to other xyloglucan molecules, which is referred to as xyloglucan endotransglucosylase (XET) activity. XTHs can also show xyloglucan hydrolase (XEH) activity. Miedes et al. (2010) found that XTH overexpression reduced xyloglucan depolymerization and softening in tomato fruit, suggesting a role of XTH in the maintenance of the structural integrity of the cell wall and that the decrease in XET activity could contribute to fruit softening. By contrast, overexpression of *Fragaria vesca FvXTH9* and *FvXTH6* in agroinfiltrated *Fragaria*  $\times$  *ananassa* fruits accelerated ripening, indicating that these genes were involved in fruit softening (Witasari et al., 2019). The XTH genes down-regulated in *FaRGLyase1* transgenic plants were not homologs to *FvXTH6* and *FvXTH9* but displayed a high identity with *FaXTH1* (Nardi et al., 2014) and *Fc-XTH1* (Opazo et al., 2010). Expression of *FaXTH1* increased during fruit development in three strawberry cvs. with contrasting firmness, reaching a peak at the 50% red stage. Bioinformatic analysis suggested that *FaXTH1* would have xyloglucan endotransglucosylase activity (Nardi et al., 2014). *Fc-XTH1* gene has also been involved in the softening of *Fragaria chiloensis* fruits (Opazo et al., 2010). As regards  $\beta$ -Xylosidase, Martínez et al. (2004) found that enzymatic activity and *FaXyl1* gene expression levels increased from green fruits to the initial stages of ripening (25–50% red), decreasing at further ripening stages. *FaXyl1* was also up-regulated in *F. vesca* fruits overexpressing the PME gene *FaPE1* (Osorio et al., 2011). The  $\beta$ -xylosidase gene up-regulated in *FaRGLyase1* plants has low homology with *FaXyl1*.

Transgenic fruits displayed other transcriptomic changes from the above described in cell wall genes. The observed changes in gene expression suggest potential alterations in various physiological processes during fruit maturation. Notably, the silencing of genes associated with lipids, proteins, and RNA metabolism may indicate a reduced activity of degradation processes, which could be associated with a decrease in senescence associated with fruit ripening. On the other hand, the overexpression of genes related to stress response and defense mechanisms suggests an activation of defense mechanisms that could also contribute to delaying senescence. Furthermore, the overexpression of genes associated with growth regulation and phytohormone metabolism may play a role in maintaining fruit quality and delaying senescence by regulating growth-related processes.

The transcriptomic changes observed in transgenic fruits suggest that *FaRGLyase1* might release cell-wall signaling molecules derived from RGI that accelerate strawberry ripening and senescence. Most studies on these signaling molecules have been focused on OGAs. These compounds are linear molecules of two to about twenty  $\alpha$ -1,4-D-galactopyranosyluronic acid (GalA) residues released upon fragmentation of HG from the primary cell wall (Ridley et al., 2001). However, little is known about oligosaccharides derived from RGI. Recently, Jiménez-Maldonado et al. (2018) found that the enzymatic degradation of RGI releases pectin fragments that induce natural defense in tomato fruit.

#### 4.5. Conclusions

The silencing of *FaRGLyase1*, the RGLyase gene most expressed in ‘Chandler’ strawberry fruit, significantly diminished the disassembly of RGI and increased the content of pectins in ripe fruits. As a result, fruit softening was reduced in transgenic lines; however, the increase in firmness obtained in these plants was less than that obtained when down-regulating HG degrading enzymes such as polygalacturonase or pectate lyase. These results indicate that the breakdown of the RGI backbone is an essential part of the cell wall disassembly process associated with fruit ripening. However, its impact on fruit texture is reduced. As observed with other cell wall genes, the silencing of *FaR-GLyase1* modified the expression of unrelated genes encoding cell wall enzymes. In this case, it is noteworthy the down-regulation of XTH genes, enzymes that have been implicated in the softening of *F. vesca* fruits. Additionally, the expression of genes involved in many other physiological processes was altered, and globally, the changes in their expression suggest that senescence was delayed in transgenic fruits. If this result is due to the higher integrity of the cell wall in transgenic ripe fruits or to the lack of RGLyase-released oligosaccharins triggering fruit senescence needs to be determined. Experiments are underway to simultaneously underregulate *FaRGLyase1* and polygalacturonase/pectate lyase to determine a possible synergistic effect on strawberry fruit texture.

#### Funding

This work was supported by MCIN (grant PID2020-118468RB-C21), by “ERDF A way of making Europe” and Consejería de Universidad, Investigación e Innovación, Junta de Andalucía (project QUAL21 012 IHSM). PR-V was awarded a Ph.D. Fellowship from Ministerio de Ciencia, Innovación y Universidades (BES-2015-073616).

#### Authors contribution

PR-V, GL-C and CP obtained and characterized transgenic plants. FJM-H, RB-P, EM performed molecular analysis. JS, JPK, SP were responsible for conducting the cell wall analyses. JM-B, AJM, and JAM designed the experiments and wrote the manuscript. All authors contributed to and approved the final draft of the manuscript.

#### Declaration of competing interest

The authors declare that they have no known competing financial interests or personal relationships that could have appeared to influence the work reported in this paper.

#### Data availability

Data will be made available on request.

#### Appendix A. Supplementary data

Supplementary data to this article can be found online at <https://doi.org/10.1016/j.plaphy.2023.108294>.

#### References

Amil-Ruiz, F., Garrido-Gala, J., Blanco-Portales, R., Folta, K.M., Muñoz-Blanco, J., Caballero, J.L., 2013. Identification and validation of reference genes for transcript normalization in strawberry (*Fragaria × ananassa*) defense responses. *PLoS One* 8. <https://doi.org/10.1371/journal.pone.0070603>.

Atkinson, R.G., Sutherland, P.W., Johnston, S.L., Gunaseelan, K., Hallett, I.C., Mitra, D., Brummell, D.A., Schröder, R., Johnston, J.W., Schaffer, R.J., 2012. Down-regulation of POLYGALACTURONASE1 alters firmness, tensile strength and water loss in apple (*Malus × domestica*) fruit. *BMC Plant Biol.* 12, 129. <https://doi.org/10.1186/1471-2229-12-129>.

Barceló, M., El-Mansouri, I., Mercado, J., Quesada, M.A., Pliego-Alfaro, F., 1998. Regeneration and transformation via *Agrobacterium tumefaciens* of the strawberry cultivar Chandler. *Plant Cell Tissue Organ Cult.* 54, 29–36.

Berumen Varela, G., Rivera Domínguez, M., Troncoso Rojas, R., Báez Sañudo, R., Tiznado Hernández, M.-E., 2017. Physiological function of rhamnogalacturonan lyase genes based in the analysis of cis-acting elements located in the promoter region. *Res. J. Biotechnol.* 12, 77–108.

Brummell, D.A., 2006. Cell wall disassembly in ripening fruit. *Funct. Plant Biol.* 33, 103–119.

Brummell, D.A., Bowen, J.K., Gapper, N.E., 2022. Biotechnological approaches for controlling postharvest fruit softening. *Curr. Opin. Biotechnol.* 78, 102786 <https://doi.org/10.1016/j.COPBIO.2022.102786>.

De Vries, J.A., Rombouts, F.M., Voragen, A.G.J., Pilnik, W., 1982. Enzymic degradation of apple pectins. *Carbohydr. Polym.* 2, 25–33. [https://doi.org/10.1016/0144-8617\(82\)90043-1](https://doi.org/10.1016/0144-8617(82)90043-1).

Edger, P.P., McKain, M.R., Yocca, A.E., Knapp, S.J., Qiao, Q., Zhang, T., 2020. Reply to: revisiting the origin of octoploid strawberry. *Nat. Genet.* <https://doi.org/10.1038/s41588-019-0544-2>.

Feng, C., Wang, J., Harris, A.J., Folta, K.M., Zhao, M., Kang, M., 2021. Tracing the diploid ancestry of the cultivated octoploid strawberry. *Mol. Biol. Evol.* 38, 478–485. <https://doi.org/10.1093/molbev/msaa238>.

Gambino, G., Perrone, I., Gribaudo, I., 2008. A Rapid and effective method for RNA extraction from different tissues of grapevine and other woody plants. *Phytochem. Anal.* 19, 520–525. <https://doi.org/10.1002/PCA.1078>.

Höfte, H., Voxeur, A., 2017. Plant cell walls. *Curr. Biol.* 27, R865–R870. <https://doi.org/10.1016/j.cub.2017.05.025>.

Jiménez-Bermúdez, S., Redondo-Navado, J., Muñoz-Blanco, J., Caballero, J.L., López-Aranda, J.M., Valpuesta, V., Pliego-Alfaro, F., Quesada, M.A., Mercado, J.A., 2002. Manipulation of strawberry fruit softening by antisense expression of a pectate lyase gene. *Plant Physiol.* 128, 751–759. <https://doi.org/10.1104/pp.010671.1>.

Jiménez-Maldonado, M.L., Tiznado-Hernández, M.E., Rascón-Chu, A., Carvajal-Millán, E., Lizardi-Mendoza, J., Troncoso-Rojas, R., 2018. Analysis of rhamnogalacturonan I fragments as elicitors of the defense mechanism in tomato fruit. *Chil. J. Agric. Res.* 78, 339–349. <https://doi.org/10.4067/S0718-58392018000300339>.

Kaczmarek, A., Pieczywek, P.M., Cybulska, J., Zdunek, A., 2022. Structure and functionality of Rhamnogalacturonan I in the cell wall and in solution: a review. *Carbohydr. Polym.* 278 <https://doi.org/10.1016/j.carbpol.2021.118909>.

Kračun, S.K., Fangel, J.U., Rydahl, M.G., Pedersen, H.L., Vidal-Melgosa, S., Willats, W.G.T., 2017. Carbohydrate microarray technology applied to high-throughput mapping of plant cell wall glycans using comprehensive microarray polymer profiling (CoMPP). *Methods Mol. Biol.* 1503, 147–165. [https://doi.org/10.1007/978-1-4939-6493-2\\_12](https://doi.org/10.1007/978-1-4939-6493-2_12).

Li, Y., Pi, M., Gao, Q., Liu, Z., Kang, C., 2019. Updated annotation of the wild strawberry *Fragaria vesca* V4 genome. *Hortic. Res.* 6, 61. <https://doi.org/10.1038/s41438-019-0142-6>.

Lin, Y., He, H., Wen, Y., Cao, S., Wang, Z., Sun, Z., Zhang, Yunting, Wang, Y., He, W., Li, M., Chen, Q., Zhang, Yong, Luo, Y., Wang, X., Tang, H., 2023. Comprehensive analysis of the pectate lyase gene family and the role of *FaPL1* in strawberry softening. *Int. J. Mol. Sci.* 24 <https://doi.org/10.3390/ijms241713217>.

Liu, T., Li, M., Liu, Z., Ai, X., Li, Y., 2021. Reannotation of the cultivated strawberry genome and establishment of a strawberry genome database. *Hortic. Res.* 8, 1–9. <https://doi.org/10.1038/s41438-021-00476-4>.

López-Casado, G., Sánchez-Raya, C., Ric-Varas, P.D., Paniagua, C., Blanco-Portales, R., Muñoz-Blanco, J., Pose, S., Matas, A.J., Mercado, J.A., 2023. CRISPR/Cas9 editing of the polygalacturonase *FaPG1* gene improves strawberry fruit firmness. *Hortic. Res.* 10 <https://doi.org/10.1093/hr/uhad011>.

Martínez, G.A., Chaves, A.R., Civeilo, P.M., 2004. Beta-xylosidase activity and expression of a beta-xylosidase gene during strawberry fruit ripening. *Plant Physiol. Biochem.* 42, 89–96. <https://doi.org/10.1016/j.plaphy.2003.12.001>.

McDonough, M.A., Kadirvelraj, R., Harris, P., Poulsen, J.-C.N., Larsen, S., 2004. Rhamnogalacturonan lyase reveals a unique three-domain modular structure for polysaccharide lyase family 4. *FEBS Lett.* 565, 188–194. <https://doi.org/10.1016/j.febslet.2004.03.094>.

Méndez-Yañez, A., González, M., Carrasco-Orellana, C., Herrera, R., Moya-León, M.A., 2020. Isolation of a rhamnogalacturonan lyase expressed during ripening of the Chilean strawberry fruit and its biochemical characterization. *Plant Physiol. Biochem.* 146, 411–419. <https://doi.org/10.1016/j.plaphy.2019.11.041>.

Miedes, E., Herbers, K., Sonnwald, U., Lorences, E.P., 2010. Overexpression of a cell wall enzyme reduces xyloglucan depolymerization and softening of transgenic tomato fruits. *J. Agric. Food Chem.* 58, 5708–5713. <https://doi.org/10.1021/jf100242z>.

Mokshina, N., Makshakova, O., Nazipova, A., Gorshkov, O., Gorshkova, T., 2019. Flax rhamnogalacturonan lyases: phylogeny, differential expression and modeling of protein structure. *Physiol. Plantarum* 167, 173–187. <https://doi.org/10.1111/ppl.12880>.

Molina-Hidalgo, F.J., Franco, A.R., Villatoro, C., Medina-Puche, L., Mercado, J.A., Hidalgo, M.A., Monfort, A., Caballero, J.L., Muñoz-Blanco, J., Blanco-Portales, R., 2013. The strawberry (*Fragaria × ananassa*) fruit-specific rhamnogalacturonate lyase 1 (*FaRGLyase1*) gene encodes an enzyme involved in the degradation of cell-wall middle lamellae. *J. Exp. Bot.* 64, 1471–1483. <https://doi.org/10.1093/jxb/ers386>.

Morales-Quintana, L., Ramos, P., Méndez-Yañez, A., 2022. Rhamnogalacturonan endolyase family 4 enzymes: an update on their importance in the fruit ripening process. *Horticulturae* 8, 465. <https://doi.org/10.3390/horticulturae8050465>.

Nardi, C.F., Villarreal, N.M., Opazo, M.C., Martínez, G.A., Moya-León, M.A., Civeilo, P.M., 2014. Expression of FaXTH1 and FaXTH2 genes in strawberry fruit. Cloning of

- promoter regions and effect of plant growth regulators. *Sci. Hortic.* 165, 111–122. <https://doi.org/10.1016/j.scienta.2013.10.035>.
- Ochoa-Jiménez, V.-A., Berumen-Varela, G., Burgara-Estrella, A., Orozco-Avitia, J.-A., Ojeda-Contreras, Á.-J., Trillo-Hernández, E.-A., Rivera-Domínguez, M., Troncoso-Rojas, R., Báez-Sañudo, R., Datsenka, T., Handa, A.K., Tiznado-Hernández, M.-E., 2018. Functional analysis of tomato rhamnogalacturonan lyase gene *Solyc11g011300* during fruit development and ripening. *J. Plant Physiol.* 231, 31–40. <https://doi.org/10.1016/J.JPLPH.2018.09.001>.
- Opazo, M.C., Figueroa, C.R., Henríquez, J., Herrera, R., Bruno, C., Valenzuela, P.D.T., Moya-León, M.A., 2010. Characterization of two divergent cDNAs encoding xyloglucan endotransglycosylase/hydrolase (XTH) expressed in *Fragaria chiloensis* fruit. *Plant Sci.* 179, 479–488. <https://doi.org/10.1016/j.plantsci.2010.07.018>.
- Osorio, S., Bombarely, A., Giavalisco, P., Usadel, B., Stephens, C., Aragüez, I., Medina-Escobar, N., Botella, M.A., Fernie, A.R., Valpuesta, V., 2011. Demethylation of oligogalacturonides by *FaPE1* in the fruits of the wild strawberry *Fragaria vesca* triggers metabolic and transcriptional changes associated with defence and development of the fruit. *J. Exp. Bot.* 62, 2855–2873. <https://doi.org/10.1093/jxb/erq465>.
- Paine, C.E.T., Marthews, T.R., Vogt, D.R., Purves, D., Rees, M., Hector, A., Turnbull, L.A., 2012. How to fit nonlinear plant growth models and calculate growth rates: an update for ecologists. *Methods Ecol. Evol.* 3, 245–256. <https://doi.org/10.1111/j.2041-210X.2011.00155.x>.
- Paniagua, C., Blanco-Portales, R., Barceló-Muñoz, M., García-Gago, J.A., Waldron, K.W., Quesada, M.A., Muñoz-Blanco, J., Mercado, J.A., 2016. Antisense down-regulation of the strawberry  $\beta$ -galactosidase gene *Fa $\beta$ Gal4* increases cell wall galactose levels and reduces fruit softening. *J. Exp. Bot.* 67, 619–631. <https://doi.org/10.1093/jxb/erv462>.
- Paniagua, C., Santiago-Doménech, N., Kirby, A.R., Gunning, A.P., Morris, V.J., Quesada, M.A., Matas, A.J., Mercado, J.A., 2017a. Structural changes in cell wall pectins during strawberry fruit development. *Plant Physiol. Biochem.* 118, 55–63. <https://doi.org/10.1016/j.plaphy.2017.06.001>.
- Paniagua, C., Kirby, A.R., Gunning, A.P., Morris, V.J., Matas, A.J., Quesada, M.A., Mercado, J.A., 2017b. Unravelling the nanostructure of strawberry fruit pectins by endo-polygalacturonase digestion and atomic force microscopy. *Food Chem.* 224, 270–279. <https://doi.org/10.1016/j.foodchem.2016.12.049>.
- Paniagua, C., Ric-Varas, P., García-Gago, J.A., López-Casado, G., Blanco-Portales, R., Muñoz-Blanco, J., Schückel, J., Knox, J.P., Matas, A.J., Quesada, M.A., Posé, S., Mercado, J.A., 2020. Elucidating the role of polygalacturonase genes in strawberry fruit softening. *J. Exp. Bot.* 71, 7103–7117. <https://doi.org/10.1093/jxb/eraa398>.
- Pedersen, S., Amtssygehus, A., 2001. Multiplex relative gene expression analysis by real-time RT-PCR using the iCycler iQ detection system. *BioRadiations* 107, 10–11.
- Posé, S., Paniagua, C., Matas, A.J., Gunning, A.P., Morris, V.J., Quesada, M.A., Mercado, J.A., 2019. A nanostructural view of the cell wall disassembly process during fruit ripening and postharvest storage by atomic force microscopy. *Trends Food Sci. Technol.* 87, 47–58. <https://doi.org/10.1016/j.tifs.2018.02.011>.
- Ridley, B.L., O'Neill, M.A., Mohnen, D., 2001. Pectins: structure, biosynthesis, and oligogalacturonide-related signaling. *Phytochemistry* 57, 929–967. [https://doi.org/10.1016/S0031-9422\(01\)00113-3](https://doi.org/10.1016/S0031-9422(01)00113-3).
- Santiago-Doménech, N., Jiménez-Bemúdez, S., Matas, A.J., Rose, J.K.C., Muñoz-Blanco, J., Mercado, J.A., Quesada, M.A., 2008. Antisense inhibition of a pectate lyase gene supports a role for pectin depolymerization in strawberry fruit softening. *J. Exp. Bot.* 59, 2769–2779. <https://doi.org/10.1093/jxb/ern142>.
- Tan, L., Eberhard, S., Pattathil, S., Warder, C., Glushka, J., Yuan, C., Hao, Z., Zhu, X., Avci, U., Miller, J.S., Baldwin, D., Pham, C., Orlando, R., Darvill, A., Hahn, M.G., Kieliszewski, M.J., Mohnen, D., 2013. An Arabidopsis cell wall proteoglycan consists of pectin and arabinoxylan covalently linked to an arabinogalactan protein. *Plant Cell* 25, 270–287. <https://doi.org/10.1105/tpc.112.107334>.
- Ulusik, S., Chapman, N.H., Smith, R., Poole, M., Adams, G., Gillis, R.B., Besong, T.M.D., Sheldon, J., Stiegelmeier, S., Perez, L., Samsulrizal, N., Wang, D., Fisk, I.D., Yang, N., Baxter, C., Rickett, D., Fray, R., Blanco-Ulate, B., Powell, A.L.T., Harding, S.E., Craigon, J., Rose, J.K.C., Fich, E.A., Sun, L., Domozych, D.S., Fraser, P. D., Tucker, G.A., Grierson, D., Seymour, G.B., 2016. Genetic improvement of tomato by targeted control of fruit softening. *Nat. Biotechnol.* 1, 1–11. <https://doi.org/10.1038/nbt.3602>.
- Vincken, J.-P., Schols, H.A., Oomen, R.J.F.J., McCann, M.C., Ulvskov, P., Voragen, A.G. J., Visser, R.G.F., 2003. If homogalacturonan were a side chain of rhamnogalacturonan I. Implications for cell wall architecture. *Plant Physiol.* 132, 1781–1789. <https://doi.org/10.1104/pp.103.022350>.
- Wang, T., Hong, M., 2016. Solid-state NMR investigations of cellulose structure and interactions with matrix polysaccharides in plant primary cell walls. *J. Exp. Bot.* 67, 503–514. <https://doi.org/10.1093/jxb/erv416>.
- Wang, D., Yeats, T.H., Ulusik, S., Rose, J.K.C., Seymour, G.B., 2018. Fruit softening: revisiting the role of pectin. *Trends Plant Sci.* <https://doi.org/10.1016/j.tplants.2018.01.006>.
- Witasari, L.D., Huang, F., Hoffmann, T., Rozhon, W., Fry, S.C., Schwab, W., 2019. Higher expression of the strawberry xyloglucan endotransglucosylase/hydrolase genes *FvXTH9* and *FvXTH6* accelerates fruit ripening. *Plant J. tpj.* 14512 <https://doi.org/10.1111/tpj.14512>.
- Xue, C., Guan, S.C., Chen, J.Q., Wen, C.J., Cai, J.F., Chen, X., 2020. Genome wide identification and functional characterization of strawberry pectin methylsterases related to fruit softening. *BMC Plant Biol.* 20, 13. <https://doi.org/10.1186/s12870-019-2225-9>.
- Yapo, B.M., 2011. Pectic substances: from simple pectic polysaccharides to complex pectins - a new hypothetical model. *Carbohydr. Polym.* 86, 373–385. <https://doi.org/10.1016/j.carbpol.2011.05.065>.
- Zhou, K., 2019. GPI-anchored SKS proteins regulate root development through controlling cell polar expansion and cell wall synthesis. *Biochem. Biophys. Res. Commun.* 509, 119–124. <https://doi.org/10.1016/J.BBRC.2018.12.081>.
- Zykwinska, A., Rondeau-Mouro, C., Garnier, C., Thibault, J.F., Ralet, M.C., 2006. Alkaline extractability of pectic arabinan and galactan and their mobility in sugar beet and potato cell walls. *Carbohydr. Polym.* 65, 510–520. <https://doi.org/10.1016/j.carbpol.2006.02.012>.